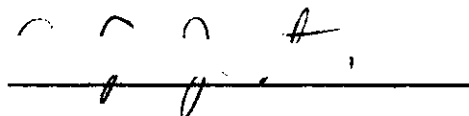


In presenting the dissertation as a partial fulfillment of the requirements for an advanced degree from the Georgia Institute of Technology, I agree that the Library of the Institution shall make it available for inspection and circulation in accordance with its regulations governing materials of this type. I agree that permission to copy from, or to publish from, this dissertation may be granted by the professor under whose direction it was written, or, in his absence, by the dean of the Graduate Division when such copying or publication is solely for scholarly purposes and does not involve potential financial gain. It is understood that any copying from, or publication of, this dissertation which involves potential financial gain will not be allowed without written permission.

A handwritten signature consisting of several loops and a final flourish, positioned above a horizontal line.

A METHOD EMPLOYING STAR BACKGROUNDS FOR IMPROVING THE ACCURACY
OF THE LOCATION OF CLOUDS OR OBJECTS IN SPACE FROM DATA RECORDED
ON FILM

A THESIS

Presented to

The Faculty of the Graduate Division

by

Carl Gerald Justus

In Partial Fulfillment

of the Requirements for the Degree

Master of Science in Physics

Georgia Institute of Technology

June 1963

54
107

A METHOD EMPLOYING STAR BACKGROUNDS FOR IMPROVING THE ACCURACY
OF THE LOCATION OF CLOUDS OR OBJECTS IN SPACE FROM DATA RECORDED
ON FILM

Approved:

91 100 - 1 1

7. 1 2

1 1 1 1

Date approved by Chairman: 5-27-63

ACKNOWLEDGMENTS

The author wishes to express his appreciation to Dr. Howard D. Edwards who directed this effort, and to the Air Force Cambridge Research Laboratories and the National Science Foundation who supplied the funds for this work under contracts AF 19(604)-5467 and NSF-G14783.

TABLE OF CONTENTS

	Page
ACKNOWLEDGMENTS	ii
LIST OF ILLUSTRATIONS	iv
SUMMARY	vi
Chapter	
I. INTRODUCTION	1
General Introduction	
The K-24 Camera and its Film Coordinate System	
Terrestrial and Celestial Coordinate Systems	
II. CAMERA FOCAL LENGTH DETERMINATION FROM THE STARS	4
III. CORRECTIONS FOR THE K-24 OR SIMILAR CAMERA SYSTEM	9
Film Shrinkage	
Light Refraction in the Glass Plate	
Camera Tilt	
Summary	
IV. CORRECTIONS FOR ATMOSPHERIC REFRACTION	25
Corrections of Star Position	
Corrections of Cloud Position	
V. MAGNITUDE OF ERRORS	32
VI. RESULTS AND CONCLUSIONS	38
APPENDIX A	41
APPENDIX B	49
APPENDIX C	53
BIBLIOGRAPHY	54

LIST OF ILLUSTRATIONS

Figure	Page
1. Coordinates on the Celestial Sphere	3
2. Typical Star Image Pair for Determining Focal Length	4
3. Star Pair Used to Determine Focal Length as They Appear on the Az-el Sphere	5
4. Right Triangles Having the Angles $\text{ARCTAN}(R_a/F)$ and $\text{ARCTAN}(R_b/F)$	7
5. The Path of a Light Ray Through the Camera	11
6. Expanded View of the Path of the Light Ray Through the Fiducial Plate	11
7. Actual and Corrected Location of an Image on the Film	15
8. The x' - y' Axes and the Camera Tilt Angle	18
9. Star Pair Used to Calculate Camera Tilt Angle, As They Appear on the Film	19
10. Star Pair Used to Determine Camera Tilt Angle, as They Appear on the Az-el Sphere	21
11. Schematic Representation of the Effects of Atmospheric Refraction in a Light Ray from a Star	25
12. Difference in True Elevations for a Star and a Body at a Finite Altitude	29
13. Angles for Measuring Angular Errors Associated with the Various Corrections	32
14. Illustration of the Intersection S and Its y' Coordinates x'_S and y'_S	41
15. Stars A' and B' with $y'_S > 0$, $x'_a > 0$, $x'_b < 0$	44
16. Stars A' and B' with $y'_S < 0$, $x'_a < 0$, $x'_b < 0$	44
17. Stars A' and B' with $y'_S < 0$, $x'_a > 0$, $x'_b < 0$	45

List of Illustrations (Cont'd.)

Figure	Page
18. Stars A' and B' with $y'_s < 0$, $x'_a > 0$, $x'_b > 0$	45
19. Stars A' and B' with $y'_s > 0$, $x'_a < 0$, $x'_b < 0$	46
20. Stars A' and B' with $y'_s > 0$, $x'_a > 0$, $x'_b > 0$	46
21. The Angle η'_a on the Az-el Sphere, and the Angle η_a on the Film	49
22. The Geometry of the Transformation of η'_a to η_a	50

SUMMARY

In research projects involving movement of clouds or objects through the upper atmosphere, position and velocity are often determined from a study of simultaneous photographs taken from two or more observing stations by either still or motion picture cameras.

The triangulation photographs have been made either at night or at twilight and hence contain a background of stars. This star background is utilized to develop a method for increasing the accuracy of the camera orientation and cloud position determinations by eliminating or correcting inherent errors in the camera system. This procedure will take into consideration the errors produced by: (1) film shrinkage, (2) light refraction in the glass plate on which the fiducial grid is ruled, and (3) misalignment (tilt) of the camera with respect to the local horizontal. In addition, a method also employing the star background is developed whereby an accurate camera focal length may be determined.

Correction for the effects of atmospheric refraction on the apparent position of stars and objects in space is available chiefly in the form of standard correction tables. Techniques and empirical formulae are developed so that correction for these effects may be accomplished analytically and thus can be programmed for a computer.

All of the correction methods mentioned are designed for use in analytic data processing with a digital computer. The methods are applicable for film measurements which require film reading accuracy to the order of a thousandth of a centimeter. By utilizing these correction

procedures the triangulation determination of the position of a body in space can be obtained to an accuracy of 0.3 milliradians angular error.

CHAPTER I

INTRODUCTION

General Introduction

The general problem considered in this research is that of determining the position (and time rate of change of position) of artificial clouds injected into the upper atmosphere at approximately 100 km altitude. To accomplish this, several observing stations were set up approximately 100-200 km apart and photographic data were taken. From these data the cloud position at any time was determined by triangulation techniques. The clouds were injected at times when the background sky was sufficiently dark that the stars in the field of view were photographable with exposure times on the order of a few seconds. This star background was used to determine the orientation in space of each of the several cameras involved in a triangulation study.

The purpose of this work was to develop a system of correction procedures designed to increase the accuracy with which camera orientation and object position in space may be determined. These procedures are especially suited for use with the K-24 camera system, but are easily adaptable to similar cameras.

The K-24 Camera and its Film Coordinate System

The K-24 is a camera equipped with a multi-element, 7 inch focal length, $f/2.5$ lens. It has a quarter-inch glass plate near the focal plane on which a fiducial grid of fine lines has been accurately ruled

1.270 cm apart. During exposure, the film is pressed against the rear surface of the fiducial plate, and a brief illumination records the grid lines on the film.

This grid system recorded on the film forms a natural x-y coordinate system in which measurements of the location of images on the film may be made. The center grid cross, near the intersection of the optical axis and the plane of the film, is taken as the origin of this system. Positive x and y are in the general directions of increasing azimuth and elevation, respectively. The origin of this system is referred to as the "center of frame."

Terrestrial and Celestial Coordinate Systems

From each of the observing stations the orientation of the cameras is determined in the azimuth-elevation, or az-el, coordinate system. Azimuth is measured east from north, and elevation is measured from the plane perpendicular to the earth radius passing through the site.

The location of stars is known in the celestial coordinate system, illustrated schematically in Figure 1. The right ascension, α , is measured eastward from γ , the vernal equinox (also called the first point of Aries). The declination, δ , is measured from the celestial equator.

The azimuth and elevation of a star from a given observation station are completely determined by knowing the right ascension and declination of the star, the time, and the latitude and longitude of the observing station. With these quantities known, the azimuth and elevation of a star can be found by a transformation of coordinates. The techniques of these coordinate transformations have been outlined in a paper by Albritten and others (1962). In the following work it will be

assumed that all of this information is known and that the necessary star azimuths and elevations have been determined.

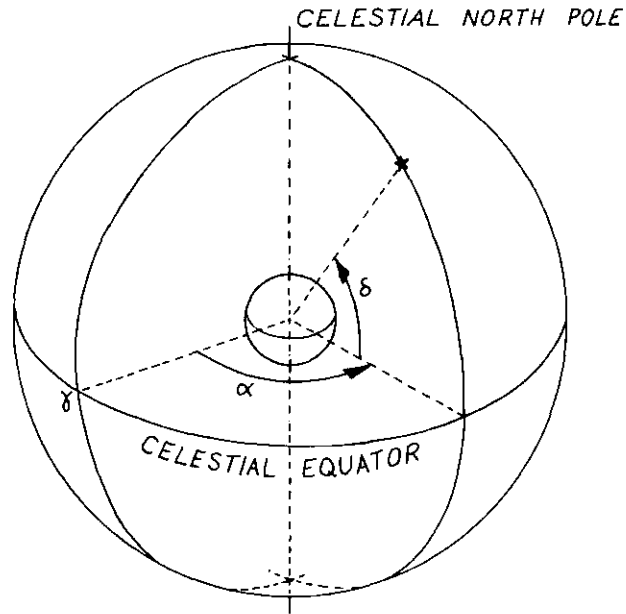


Figure 1. Coordinates on the Celestial Sphere

CHAPTER II

CAMERA FOCAL LENGTH DETERMINATION FROM THE STARS

In order to utilize measurements of image position on the film, the focal length of the camera lens must be accurately known. The focal length of a camera lens may be determined from two star images appearing on the film. A typical pair of images, A and B, is shown in Figure 2. They are located at radial distances R_a and R_b from the center of frame, O, and are separated from each other by a distance ΔR . Angle AOB is called Q.

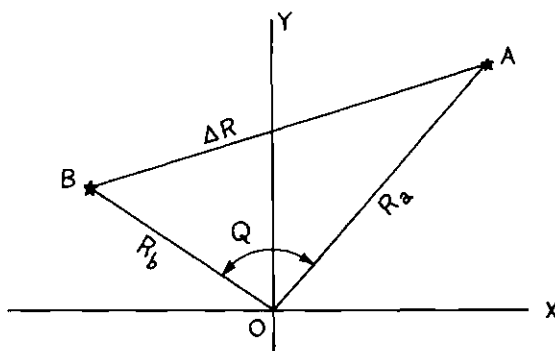


Figure 2. Typical Star Image Pair for Determining Focal Length

Figure 3 shows the same pair of stars (now labeled A' and B') as they appear on the az-el sphere, which is an imaginary sphere, centered at the observing site, and considered to have an infinite radius similar to the celestial sphere. They form a spherical triangle A'B'Z with the

zenith, which is the point at which an earth radius through the observing site intersects with the az-el sphere. Sides c_a and c_b of this spherical triangle are the complements of the elevations of A' and B' , respectively. The difference in the azimuths of the two stars is angle ΔA . The sides of the spherical triangle formed by the two stars and the projection of the center of frame onto the az-el sphere are q , a , and b , as shown. Angle $A'O'B'$ is called Q' .

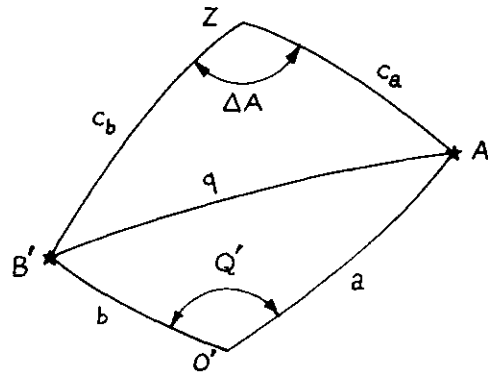


Figure 3. Star Pair Used to Determine Focal Length as They Appear on the Az-el Sphere

From the spherical triangle $A'B'Z$:

$$\cos(q) = \cos(c_a)\cos(c_b) + \sin(c_a)\sin(c_b)\cos(\Delta A) \quad (1)$$

Since all quantities on the right of (1) are known, $\cos(q)$ is known.

The angles a and b are given by

$$a = \text{ARCTAN}(R_a/F) \text{ and } b = \text{ARCTAN}(R_b/F) , \quad (2)$$

where F is the focal length of the lens (yet to be determined).

Since the center of frame may be considered to be on the optical axis, and since Q' is measured in a plane perpendicular to this axis

$$Q' = Q$$

Employing the law of cosines on the plane triangle AOB provides a relation for $\cos(Q)$

$$\cos(Q) = \frac{R_a^2 + R_b^2 - (\Delta R)^2}{2R_a R_b} \quad (3)$$

thus determining $\cos(Q)$ in terms of known quantities.

Applying the "law of cosines" for spherical trigonometry to the spherical triangle A'O'B':

$$\cos(q) = \cos(a)\cos(b) + \sin(a)\sin(b)\cos(Q) \quad (4)$$

The terms $\cos(q)$ and $\cos(Q)$ are known from equations (1) and (3). Substituting equations (2) into (4)

$$\begin{aligned} \cos(q) = & \cos[\text{ARCTAN}(R_a/F)] \cos[\text{ARCTAN}(R_b/F)] \\ & + \sin[\text{ARCTAN}(R_a/F)] \sin[\text{ARCTAN}(R_b/F)] \cos(Q) \end{aligned} \quad (5)$$

Considering the triangles shown in Figure 4, it is evident that substitutions may be made for the sines and cosines involving F in the right side of (5).

Making these substitutions yields

$$\cos(q) = \frac{F}{(R_a^2 + F^2)^{\frac{1}{2}}} \frac{F}{(R_b^2 + F^2)^{\frac{1}{2}}} + \frac{R_a}{(R_a^2 + F^2)^{\frac{1}{2}}} \frac{R_b}{(R_b^2 + F^2)^{\frac{1}{2}}} \cos(Q)$$



Figure 4. Right Triangles Having the Angles
 $\text{ARCTAN}(R_a/F)$ and $\text{ARCTAN}(R_b/F)$

F is now the only unknown and it may therefore be solved for in the following manner:

$$\cos(q)[(R_a^2 + F^2)(R_b^2 + F^2)]^{\frac{1}{2}} = F^2 + R_a R_b \cos(Q). \quad (6)$$

Squaring both sides of (6), one obtains

$$\begin{aligned} \cos^2(q)(R_a^2 + F^2)(R_b^2 + F^2) &= F^4 + 2F^2 R_a R_b \cos(Q) \\ &+ R_a^2 R_b^2 \cos^2(Q), \end{aligned}$$

which becomes, after a combination of terms,

$$\begin{aligned} F^4[\cos^2(q) - 1] + F^2[(R_a^2 + R_b^2)\cos^2(q) - 2R_a R_b \cos(Q)] \\ + [\cos^2(q) - \cos^2(Q)]R_a^2 R_b^2 = 0. \end{aligned}$$

Now let

$$U = \cos^2(q) - 1 , \quad (7)$$

$$V = [(R_a^2 + R_b^2) \cos^2(q) - 2R_a R_b \cos(Q)] ,$$

$$W = [\cos^2(q) - \cos^2(Q)] R_a^2 R_b^2 ,$$

then

$$UF^4 + VF^2 + W = 0 ,$$

which, when solved for F^2 by the quadratic formula, yields

$$F^2 = \frac{-V \pm (V^2 - 4UW)^{\frac{1}{2}}}{2U} ,$$

so that F is given by

$$F = \left[\frac{-V \pm (V^2 - 4UW)^{\frac{1}{2}}}{2U} \right]^{\frac{1}{2}} . \quad (8)$$

Equation (8) gives two values for F . In practice both positive and negative roots may be considered and the value of F with the minimum deviation from the nominal focal length taken as the correct value.

CHAPTER III

CORRECTIONS FOR THE K-24 OR SIMILAR CAMERA SYSTEM

Film Shrinkage

The film was found to shrink during the time between its exposure and analysis; consequently, this shrinkage must be taken into consideration when measurements taken from the film are used in calculations. Analytic correction is precluded because the shrinkage is not consistent between successive exposures on the same roll of film, nor does the shrinkage occur in any regular fashion over each individual exposure.

The fiducial grid superimposed on each exposure, besides its primary purpose of providing a film coordinate system, serves the secondary purpose of permitting the film shrinkage to be calculated and corrected for.

Image displacement is assessed by counting 1.270 cm increments, the nominal distance between grid lines, then measuring distances to the nearest fiducial lines in both x and y directions. If the procedure is carried no further, the effects of shrinkage will be confined to one fiducial square. Further reduction of the effects of film shrinkage may be obtained by measuring the dimensions of the fiducial square in which the image is located and using a linear interpolation process to correct for the image location within the fiducial square.

To check the accuracy of the spacing of the ruled lines on the plates several measurements of their separation were made. The mean distance between fiducial lines was found to be 1.2697 ± 0.0004 (rms) cm.

Several measurements of the film shrinkage between consecutive fiducial lines showed a mean shrinkage of 0.003 cm, with a maximum of about 0.006 cm and a minimum of zero. For the K-24 camera system 0.001 cm amounts to 0.055 milliradian, which corresponds to 8 meters at 150 km range.

Light Refraction in the Fiducial Plate

Although the glass fiducial plate allows for the elimination of errors caused by film shrinkage, it introduces another error into the measurements taken from the film: light refraction in the glass plate. Unlike film shrinkage, this error can be evaluated analytically.

Figure 5 shows a light ray entering the camera with an angle of incidence β measured from the optical axis. If the plate were not present the ray would strike the film (which is pressed against the back of the plate) at a distance ρ from the optical axis. Since the light ray is refracted in the plate, it actually strikes the film at a distance r from the optical axis. The angle of refraction is λ , shown in the expanded view in Figure 6, and $\phi = \beta - \lambda$. The focal length, F , is the distance from the nodal point of the lens to the rear of the fiducial plate, t is the thickness of the glass plate, and n is the index of refraction in the glass plate.

By Snell's Law

$$n \sin(\lambda) = \sin(\beta) \quad (9)$$

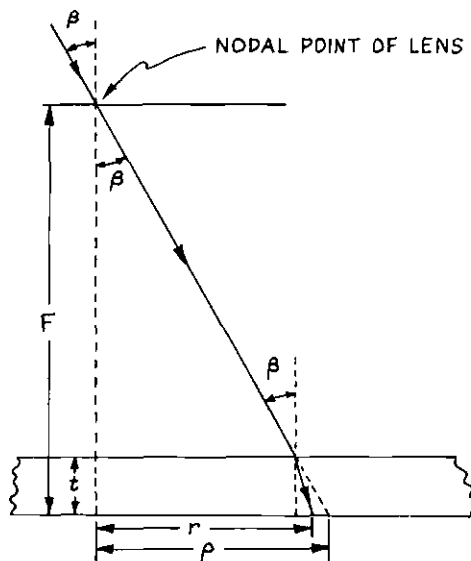


Figure 5. The Path of a Light Ray Through the Camera

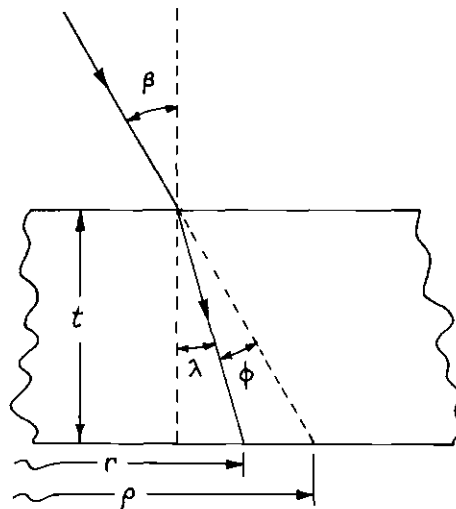


Figure 6. Expanded View of the Path of the Light Ray Through the Fiducial Plate

From inspection of Figure 5

$$\sin(\beta) = \frac{\rho}{(\rho^2 + F^2)^{\frac{1}{2}}} \quad (10)$$

$$\tan(\beta) = \rho/F \quad (11)$$

Substituting (9) into (10) yields

$$\sin(\lambda) = \frac{\rho}{n(\rho^2 + F^2)^{\frac{1}{2}}} \quad (12)$$

Using the identity $\cos(\lambda) = (1 - \sin^2 \lambda)^{\frac{1}{2}}$

$$\cos(\lambda) = \frac{[n^2(\rho^2 + F^2) - \rho^2]^{\frac{1}{2}}}{n(\rho^2 + F^2)^{\frac{1}{2}}} \quad (13)$$

Dividing (12) by (13) gives

$$\tan(\lambda) = \frac{\rho}{[n^2(\rho^2 + F^2) - \rho^2]^{\frac{1}{2}}} \quad (14)$$

But from inspection of Figure 5

$$\frac{r - t \tan(\lambda)}{F - t} = \tan(\beta) = \rho/F \quad (15)$$

Therefore from (15)

$$r = \rho + t[\tan(\lambda) - \rho/F] \quad (16)$$

Substituting (14) into (16)

$$r = \rho + \frac{t\rho}{F} \left(\frac{F}{[n^2(\rho^2 + F^2) - \rho^2]^{\frac{1}{2}}} - 1 \right) \quad (17)$$

Letting $J^2 = \frac{n^2 - 1}{n^2 F^2}$

$$r = \rho + \frac{t\rho}{F} \left(\frac{1}{n(1 + J^2 \rho^2)^{\frac{1}{2}}} - 1 \right) \quad (18)$$

Expanding the radical in (18) in a power series

$$r = \rho + \frac{t}{F} \left(-1 + \frac{1}{n} (1 - J^2 \rho^2 + \frac{3}{8} J^4 \rho^4 - \frac{5}{16} J^6 \rho^6 + \dots) \right) \quad (19)$$

Equation (19) is a series expansion of r in terms of ρ . By the method of reversion of series (cf. CRC Standard Mathematical Tables), ρ may be found as a series expansion in terms of r . Let

$$a_1 = 1 - \frac{t}{F} (1 - 1/n) \quad (20)$$

$$a_3 = -\frac{1}{2} \frac{t}{Fn} J^2$$

$$a_5 = \frac{3t}{8Fn} J^4$$

$$a_7 = -\frac{5t}{16Fn} J^6$$

then

$$\rho = A_1 r + A_3 r^3 + A_5 r^5 + A_7 r^7 + \dots \quad (21)$$

where the first few A coefficients are given by

$$A_1 = 1/a_1 \quad A_3 = -\frac{a_3}{a_1^4} \quad (22)$$

$$A_5 = (3a_3^3 - a_1 a_5) / a_1^7$$

$$A_7 = (8a_1 a_3 a_5 - a_1^2 a_7 - 12a_3^3) / a_1^{10}$$

The actual quantity of interest is not ρ , however, but the change in position, C , of the image, which is $\rho - r$. Therefore from (21)

$$C = (A_1 - 1)r + A_3 r^3 + A_5 r^5 + A_7 r^7 + \dots \quad (23)$$

The A coefficients are determined by equations (22) and (20) and depend only on n , t , and F . The index of refraction and thickness for each glass plate may be measured and used separately. However, measurements of n for several plates yielded a value of 1.524 indicating that this may be used as the value for all plates. The thickness of the plates was found to vary by about 10 per cent from plate to plate, so that separate plate thickness values are used. If the accurate focal length has been determined by the method previously described, it may be used in the formulas for determining the A coefficients. However, since these formulas do not vary rapidly with F , if the focal length is known to within about ± 2 mm (for the K-24, 7 inch lens) the A coefficients determined from such a value will still be quite adequate. For example, if $r = 6$ cm, C would be altered about one per cent for a 2 mm change in the focal length value used in the calculation.

If a value of displacement of an image from the center of frame is to be corrected for plate refraction, the relation is

$$\rho = r + C$$

where ρ is the corrected radial distance of the image from the center of frame, r is the observed radial distance and C is given by (23).

Figure 7 illustrates an image and its corrected location on the film.

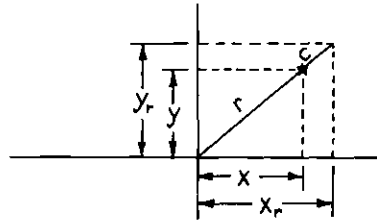


Figure 7. Actual and Corrected Location of an Image on the Film

To find the corrected values of x and y (x_r and y_r) the relations

$$x_r/x = \rho/r \quad \text{and} \quad y_r/y = \rho/r$$

are used. Therefore

$$x_r = x(\rho/r) = x\left(\frac{r+C}{r}\right)$$

$$\text{or} \quad x_r = x(1 + C/r) \quad (24)$$

and similarly

$$y_r = y(1 + C/r) \quad (25)$$

If (23) is substituted into (24) and (25)

$$x_r = x(A_1 + A_3r^2 + A_5r^4 + A_7r^6 + \dots) \quad (26)$$

$$y_r = y(A_1 + A_3r^2 + A_5r^4 + A_7r^6 + \dots)$$

Equations (26) are not exactly correct if the center of frame does not coincide with the intersection of the optical axis and the plane of the film. If the displacement of the center of frame from the optical axis is known, a new film coordinate system may be set up with the origin on the optical axis, and the values of x and y converted into the new system by translation. Equations (26) would then be correct with the values of x and y so altered. However, if the displacement of the center of frame from the optical axis is of the order of 2 mm, as indicated in the K-24 instruction manual (Vitro, 1954), the error caused by neglecting this coordinate translation is on the order of 0.002 cm for the K-24 system. This assumes that the only error introduced by neglecting the translation is the error in evaluating the refraction C . That is, for a deviation, δ , of the center of frame from the optical axis $C(r + \delta) - C(r)$ is about 0.002 cm for $\delta = 2\text{mm}$.

Although no direct measurements of the deviation of the center of frame from the optical axis have been made, tests have been made which show that no observable systematic radial error is still present after the plate refraction corrections have been applied but without correcting for displacement of the center of frame from the optical axis. The negative results of these tests also show that the radial distortion of the lens is too small to be taken into consideration.

Equations (26) may also be reduced in terms to give any desired degree of accuracy. In fact, if the terms in r^4 and higher powers of r are neglected, giving the simple formulas

$$x_r = x(A_1 + A_2 r^2) \quad (27)$$

$$y_r = y(A_1 + A_2 r^2)$$

the corrected coordinates obtained from these formulas will be accurate to about 0.001 cm at $r = 9$ cm.

Camera Tilt

Referring to Figure 3, it is apparent that a line $O'Z$, connecting the zenith with the projection of the center of frame onto the az-el sphere, should correspond to the positive y axis when projected onto the film. However, due to several causes for which it is either impossible or impractical to compensate, this projection of $O'Z$ may not correspond to the y axis on the film. In such a case a new $x'-y'$ film coordinate system, shown in Figure 8, could be formed by a rotation of the $x-y$ coordinates through an angle θ , so that the projection of $O'Z$ would correspond to the y' axis.

It is advantageous to know the angle θ , called the camera tilt angle, so that the calculations of line of sight to the cloud or object being photographed may be carried out in the $x'-y'$ coordinates. Note, however, that the camera tilt angle does not affect calculations which depend only on the radial distance from the center of frame, such as the

fiducial plate refraction corrections and the focal length calculations.

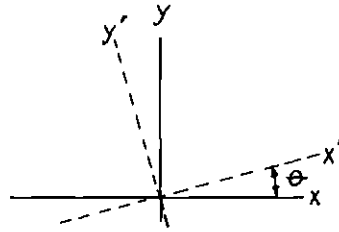


Figure 8. The x' - y' Axes and the Camera Tilt Angle

The camera tilt angle may be calculated by considering a pair of stars, A and B shown in Figure 9, as their images appear on the film. The images of A and B are located at radial distances R_a and R_b from the center of frame, 0; they are separated by a distance ΔR . Point M is the intersection of ΔR and the y' axis. The angle between AM and the y' axis is η_a , and the angle between BM and the y' axis is η_b .

If the coordinates in the x - y system of stars A and B are x_a, y_a and x_b, y_b then the x' - y' coordinates of A and B are x'_a, y'_a and x'_b, y'_b given by

$$x'_a = x_a \cos(\theta) + y_a \sin(\theta)$$

$$x'_b = x_b \cos(\theta) + y_b \sin(\theta)$$

$$y'_a = y_a \cos(\theta) - x_a \sin(\theta)$$

$$y'_b = y_b \cos(\theta) - x_b \sin(\theta)$$

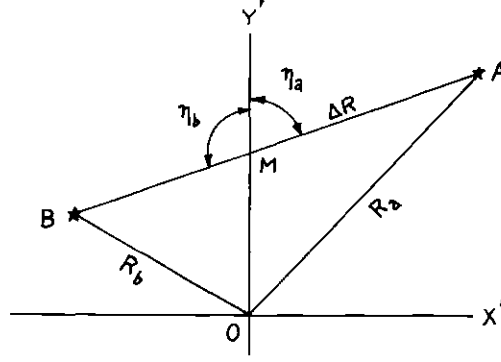


Figure 9. Star Pair Used to Calculate Camera Tilt Angle, As They Appear on the Film

Letting $\Delta x' = x'_a - x'_b$ and $\Delta y' = y'_a - y'_b$ one has

$$\Delta x' = \Delta x \cos(\theta) + \Delta y \sin(\theta) \quad (28)$$

$$\Delta y' = \Delta y \cos(\theta) - \Delta x \sin(\theta)$$

where $\Delta x = x_a - x_b$ and $\Delta y = y_a - y_b$.

The slope, y'_x , of the line joining A and B on the film is $\Delta y' / \Delta x'$ in the x' - y' coordinates. Therefore, using the values of $\Delta x'$ and $\Delta y'$ in (28), one obtains

$$y'_x = \frac{\Delta y \cos(\theta) - \Delta x \sin(\theta)}{\Delta x \cos(\theta) + \Delta y \sin(\theta)} ,$$

which, when solved for θ , yields

$$y'_x [\Delta x \cos(\theta) + \Delta y \sin(\theta)] = \Delta y \cos(\theta) - \Delta x \sin(\theta)$$

$$\sin(\theta) [\Delta x + \Delta y(y'_x)] = \cos(\theta) [\Delta y - \Delta x(y'_x)]$$

$$\theta = \text{ARCTAN} \left[\frac{\Delta y - \Delta x(y'_x)}{\Delta x + \Delta y(y'_x)} \right] . \quad (29)$$

Relation (29) provides a determination of the camera tilt angle if y'_x is known. The slope y'_x is determined by the value of the angles η_a or η_b by the relations^{*}

$$y'_x = \tan(\pi/2 - \eta_a) \quad (30)$$

$$y'_x = \tan(\eta_b - \pi/2)$$

Either of relations (30) may be used in (29) to determine θ , or both relations (30) may be used to give separate values of θ which may be averaged.

To determine the values of η_a and η_b , consider the stars A and B as seen on the az-el sphere, shown in Figure 10 as A' and B'. The coelevations of A' and B' are c_a and c_b . The coelevation of the projection of the center of frame onto the az-el sphere, O', is c_o . Point M' and the sides q, a, and b of the spherical triangle A'B'O' are the projections onto the az-el sphere of M, ΔR , R_a , and R_b , respectively, from Figure 9. Several angles of the spherical triangles formed are also

* See Appendix A

$$\cos(\xi_a) = \frac{\cos(b) - \cos(a) \cos(q)}{\sin(q) \sin(a)} \quad (32)$$

From Figure 10 the relation for $\cos \psi_a$ is

$$\cos \psi_a = \cos(v_a + \xi_a) \quad (33)$$

With the value of $\cos \psi_a$ determined, the spherical triangle $A'ZO'$ may be solved for side c_o and angle ζ_a .

$$\cos(c_o) = \cos(c_a) \cos(a) + \sin(c_a) \sin(a) \cos(\psi_a) \quad (34)$$

$$\cos(\zeta_a) = \frac{\cos(a) - \cos(c_o) \cos(c_a)}{\sin(c_o) \sin(c_a)} \quad (35)$$

From spherical triangle $ZA'M'$

$$\cos(\eta'_a) = -\cos(v'_a) \cos(\zeta_a) + \sin(v'_a) \sin(\zeta_a) \cos(c_a) \quad (36)$$

where in the case shown in Figure 10

$$v'_a = v_a \quad (37)$$

It should be noted that (33) and (37) apply only for the case shown in Figure 10. See Appendix A for equations to be used instead of (33) and

(37) for cases other than that shown in Figure 10.

Side ZM' of the spherical triangle $ZA'M'$, called d in Figure 10 may be found.

$$\sin(d) = \frac{\sin(c_a) \sin(v'_a)}{\sin(\eta'_a)} \quad (38)$$

The angle ω between the lines from the observing site to M' and to O' (side $O'M'$ of the spherical triangle $O'M'A'$) is given by

$$\omega = c_o - d \quad (39)$$

This angle ω relates the angle η'_a on the az-el sphere to the angle η_a on the film through the relation

$$\tan(\eta_a) = \tan(\eta'_a) \cos(\omega) \quad (40)$$

derived in Appendix B.

Equation (40) determines η_a , so that the slope y'_x is now determined by (30) and the camera tilt angle θ is given by (29).

Relations (31) through (40) have been a method of evaluating η_a from the spherical triangles and angles associated with star A' in Figure 10. A similar procedure for evaluating η_b may be carried out with the spherical triangles and angles associated with star B' , by substituting the appropriate counterpart angles and sides of spherical triangles

into (31) through (40).

With the camera tilt angle determined, coordinates x and y may be converted to x' and y' by the relations

$$x' = x \cos(\theta) + y \sin(\theta) \quad (41)$$

$$y' = y \cos(\theta) - x \sin(\theta)$$

All of the pertinent calculations have been made for determining the azimuth and elevation of the line of sight along the optical axis of the camera. See Appendix C for the methods of obtaining these quantities.

Summary

Chapter III has provided techniques which allow for the correction of the effects due to film shrinkage, light refraction in the glass fiducial plate, and camera tilt. The effects of displacement of the center of frame from the optical axis, and the radial distortion in the lens, have not been corrected for, but evidence has been offered to show that these effects are indeed negligible.

CHAPTER IV

CORRECTIONS FOR ATMOSPHERIC REFRACTION

Corrections of Star Position

The path of a light ray passing from free space to the surface of the earth is deviated from a straight line because of the index of refraction of the atmosphere. Because this refractive index varies not only with height above the earth but with temperature and pressure at the surface of the earth, this deviation is not a simply derived quantity.

If the assumption is made that the atmosphere has a spherically stratified index of refraction, the deviation will depend on the elevation of the line of sight to the light source (or equivalently on the zenith angle, z , the complement of the elevation), but will not depend on the azimuth. Figure 11 shows schematically the effects of atmospheric refraction on the path of a light ray coming from a star considered to be at infinity. Here z is the apparent zenith angle, ζ is the true zenith angle, and r is the angular change in the apparent position of the star due to atmospheric refraction.

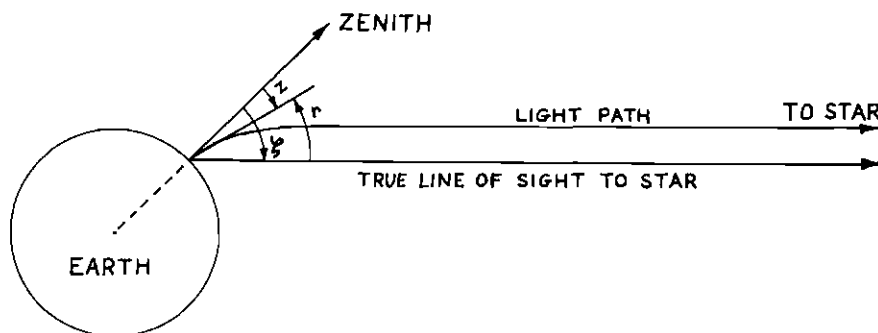


Figure 11. Schematic Representation of the Effects of Atmospheric Refraction on a Light Ray from a Star

Bessel's refraction table (Chauvenet, 1960) provides numerical evaluation of r for various temperatures, pressures, and zenith angles. This table is based on the formula

$$r(z) = \alpha \beta^A \gamma^\lambda \tan(z) \quad (42)$$

where

$$\beta = B T \quad (43)$$

and gives the values of α , B , T , A , γ and λ . The quantities α , A and λ are functions of z ; T and γ are functions of temperature; B is a function of pressure.

If the apparent zenith angle is known and one wishes to obtain the true zenith angle,

$$\zeta = z + r(z) \quad (44)$$

is used. If the true zenith angle is known it is more convenient to know r as a function of ζ so that the relation

$$z = \zeta - r(\zeta) \quad (45)$$

may be used. Based on the formula

$$r(\zeta) = \alpha' \beta'^A \gamma'^\lambda \tan(\zeta) \quad (46)$$

Bessel's table also gives values for α' , A' , and λ' as functions of ζ .

Bessel's table is in a convenient form for hand calculations of the effects of atmospheric refraction. But for the handling of large quantities of data, expressions for the various factors in terms of fairly simple functions which could be put into a computer program would be advantageous.

A least squares polynomial fit of the data from Bessel's table gave for γ , B , and T :

$$\gamma = 1.10553 - 2.3904 \times 10^{-3} \theta + 4.987 \times 10^{-6} \theta^2 - 7.55 \times 10^{-9} \theta^3 \quad (47)$$

$$B = 0.337874 p \quad (48)$$

$$T = 1.00288 - 8.944 \times 10^{-5} \theta \quad (49)$$

where θ is the temperature in degrees Fahrenheit and p is the atmospheric pressure at the surface of the earth in inches of mercury.

The form $K_1 + K_2 \tan^n(z)$ was assumed for α , A and λ , where K_1 and K_2 are constant and n is a function of z (or a constant). This assumption, and trial and error procedures to determine the constants and exponent, led to

$$\alpha = 57.751 - 0.07[\tan(z)]^{1.96} \quad (50)$$

$$A = 1 + 2.15 \times 10^{-4} [\tan(z)]^{1.7} \quad (51)$$

$$\lambda = 1 + 0.0018 \tan(z) [1 - 0.821 \sin^2(9z/7.4)] \quad (52)$$

The assumption of the form $K_1 + K_2 \tan^n(\xi)$ for α' , A' , and λ' , led to

$$\alpha' = 57.734 - 0.0084 [\tan(\xi)]^{1.97} \quad (53)$$

$$A' = 1 - 2.15 \times 10^{-4} [\tan(\xi)]^{1.7} \quad (54)$$

$$\lambda' = 1 + 0.0013 [\tan(\xi)]^{1.4} + 0.4525(S + |S|) \quad (55)$$

where S is $\sin \frac{9(\xi - 45)}{2.9}$

Using the factors as given above in (42) or (46) gives r in seconds of arc. The expressions (47) through (55) reproduce the values in Bessel's refraction table over the range $0^\circ \leq z < 75^\circ$ to within an accuracy of about 0.01 second of arc. In the range $75^\circ \leq z < 80^\circ$ the accuracy is good to about 0.5 seconds of arc.

For stars it is the true zenith angle ξ which is known. But the stars are seen, and show up on the film at their apparent zenith angle z . Therefore (46) and (45) are used to correct for star position.

For bodies such as the artificial clouds mentioned in the introduction, the apparent elevation is known. However, for triangulation purposes one needs to know the true elevation, or zenith angle. Equations (42) and (44) are used for this, as will be explained more fully in the following section.

Corrections of Cloud Position

The formulas of the previous section apply to stars or other bodies which can be considered at an infinite distance from the observing site. The corrections for the effects of atmospheric refraction on the apparent zenith angle of an object close to the earth are actually dependent on the height of the body above the earth's surface.

Figure 12 shows that an object, such as the artificial cloud mentioned in the introduction, which has the same apparent elevation as a star would not have the same true elevation as the star.

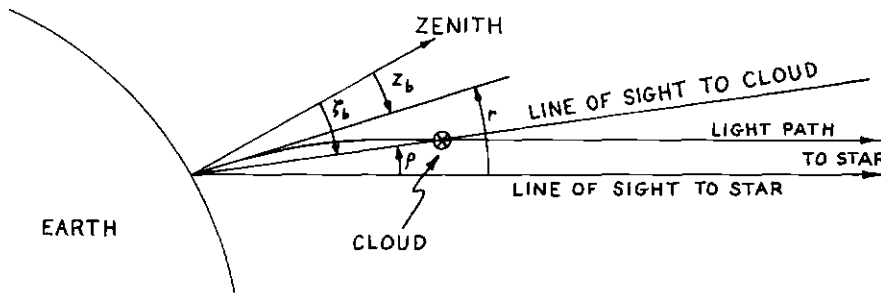


Figure 12. Difference in True Elevations for a Star and a Body at a Finite Altitude

The angle ρ shown in Figure 12 is the difference in the true zenith angles of the body and the star. The true zenith angle, ζ_b , of the body can be found from the apparent zenith angle, z_b , by the relation

$$\zeta_b = z_b + r(z) - \rho(z) \quad (56)$$

The function $r(z)$ is the correction found previously by relation (42) and its associated equations (47) through (52).

Tabulated values of $\rho(z)$ for various heights above the earth were

found (Jones, 1961). These values are based on the same assumption as that for the star corrections, namely a spherically stratified index of refraction in the atmosphere. Also it is assumed that the index of refraction between the body and the stars is unity. A nominal value is assumed for the index of refraction of air at sea level and for the radius of the earth.

It is also desirable to have equations for the function $\rho(z)$ instead of the tabulated values. An approximation for finding $\rho(z)$ for any height h was found to be

$$\rho(z) = \frac{105.4}{h} \rho_{100}(z) \quad (57)$$

where $\rho_{100}(z)$ is the ρ function evaluated at a height of 100 km.

The assumption of the form $A \tan(z) + f(z)$ for ρ_{100} and trial and error evaluation of the constant A and the values of the function $f(z)$ led to the relation

$$\rho_{100}(z) = 5.59 \tan(z) + 4.23 \left[1 - \frac{(z-36)^2}{1296} \right] + \Delta(z) \quad (58)$$

where

$$\Delta(z) = -0.29 \left| \sin(3z) \right| \quad z \leq 60^\circ \quad (59)$$

$$\Delta(z) = 0.28 \left(\frac{z-60}{10} \right)^{2.87} \quad 60^\circ < z \leq 80^\circ \quad (60)$$

All of these constants are in the necessary dimensions to calculate $\rho(z)$ in seconds of arc. Formulas (58) through (60) will reproduce the values of $\rho(z)$ in the tables to within 0.03 seconds of arc for $h = 100$ km. Formula (57) coupled with these formulas will reproduce the values for $\rho(z)$ at $h = 200$ km to within about 0.1 second of arc $0^\circ \leq z < 80^\circ$.

CHAPTER V

MAGNITUDE OF ERRORS

In dealing with the magnitude of the errors discussed previously it is convenient to express them in terms of angular error. Refraction in the glass plate produces error which is solely radial in nature, that is, along the radius from the center of frame. But camera tilt leads to error which is associated with the perpendicular to the radius from the center of frame.

Therefore it is suitable to express angular errors in terms of $\Delta\alpha$ and $\Delta\phi$ where α is measured along the radius and ϕ is measured along the perpendicular to the radius. The angles α and ϕ are illustrated in Figure 13, where F is the focal length of the camera, R is the radius to the point at which the error is evaluated, and S is the distance on the film plane associated with the angle $\Delta\phi$.

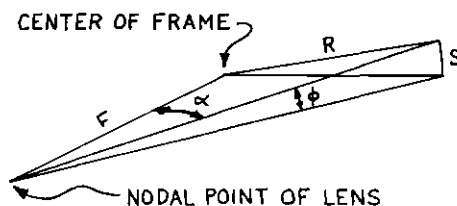


Figure 13. Angles for Measuring Angular Errors Associated With the Various Corrections

The angle α is determined by

$$\tan \alpha = R/F \quad (61)$$

and ϕ , which is considered small, is given in radians by

$$\phi = \frac{S}{(R^2 + F^2)^{\frac{1}{2}}} \quad (62)$$

Inaccuracy in the determination of the focal length of the camera will lead to error in α . From (61)

$$\sec^2 \alpha \Delta \alpha = - \frac{R}{F^2} \Delta F$$

$$\frac{\Delta \alpha}{\Delta F} = - \frac{R}{F^2 (\sec^2 \alpha)} = - \frac{R}{F^2 (1 + \tan^2 \alpha)},$$

which becomes, upon the substitution of R/F for $\tan \alpha$

$$\frac{\Delta \alpha}{\Delta F} = - \frac{R}{F^2 + R^2} \quad (63)$$

The uncertainty in α , $\delta \alpha_f$ caused by an uncertainty δF would then be

$$\delta \alpha_f = \left| \frac{\Delta \alpha}{\Delta F} \right| \delta F \quad (64)$$

Values of $\left| \Delta \alpha / \Delta F \right|$ are given in Table 1.

For errors producing uncertainty in R , formula (61) is again employed to obtain

$$\sec^2 \alpha \Delta \alpha = \frac{1}{F} \Delta R \quad (65)$$

$$\frac{\Delta \alpha}{\Delta R} = \frac{1}{F(\sec^2 \alpha)} = \frac{1}{F(1 + \tan^2 \alpha)}$$

$$\frac{\Delta \alpha}{\Delta R} = \frac{F}{F^2 + R^2} \quad (66)$$

The uncertainties in α , $\delta \alpha_s$ and $\delta \alpha_r$, caused by film shrinkage and refraction in the glass would be

$$\delta \alpha_s = \frac{\Delta \alpha}{\Delta R} \delta R_s \quad (67)$$

$$\delta \alpha_r = \frac{\Delta \alpha}{\Delta R} \delta R_r \quad (68)$$

where δR_s and δR_r are the uncertainties in R caused by shrinkage and refraction respectively. Here $\delta \alpha_s$ is the error in α caused by film shrinkage if one does not read the position of a point on the film by counting fiducial square increments as mentioned in the section on film shrinkage. Values of $\Delta \alpha / \Delta R$, δR_s , $\delta \alpha_s$, δR_r , and $\delta \alpha_r$ are given in Table 1.

For error caused by tilt, formula (62) is used to obtain

$$\Delta \phi = \frac{\Delta S}{(R^2 + F^2)^{\frac{1}{2}}} \quad (69)$$

$$\frac{\Delta \phi}{\Delta S} = \frac{1}{(R^2 + F^2)^{\frac{1}{2}}}$$

The error in ϕ , $\delta\phi_\theta$, caused by an uncertainty in S , δS_θ , would be given by

$$\delta\phi_\theta = \frac{\Delta\phi}{\Delta S} \delta S_\theta \quad (70)$$

Values of δS_θ per degree of tilt, and $\delta\phi_\theta$ are given in Table 1.

Note that film shrinkage also produces an error in S and a ϕ component of film shrinkage could be evaluated. However, it is evident from Table 1 that since $\Delta\phi/\Delta R$ and $\Delta\phi/\Delta S$ are almost equal, the two components of film shrinkage error will also be approximately equal.

All values in Table 1 are based on a focal length of 18.14 cm (7.140 inches) which was found to be the average focal length of the K-24 cameras. All angles in Table 1 are in milliradians (mr.).

For comparison Table 2 shows the corrections for atmospheric refraction (in milliradians) for several values of zenith angle, z .

Table 1. Magnitude of Errors for Various Values of R

	R=0 cm	R=3 cm	R=6 cm	R=9 cm
$\left \frac{\Delta \alpha}{\Delta F} \right \left(\frac{\text{mr}}{\text{cm}} \right)$	0	9	17	22
$\frac{\Delta \alpha}{\Delta R} \left(\frac{\text{mr}}{\text{cm}} \right)$	55	54	51	44
$\frac{\Delta \phi}{\Delta S} \left(\frac{\text{mr}}{\text{cm}} \right)$	55	54	52	50
δR_s (cm) (Average)	0	0.007	0.014	0.021
$\delta \alpha_s$ (mr)	0	0.38	0.75	0.93
δR_r (cm)	0	0.031	0.067	0.111
$\delta \alpha_r$ (mr)	0	1.6	3.4	4.9
$\delta S_\theta \left(\frac{\text{cm}}{\text{cm}} \right)$	0	0.052	0.105	0.158
$\delta \phi_\theta$ (mr) ($\theta = 1^\circ$)	0	2.8	5.5	7.9

Table 2. Corrections for Atmospheric Refraction
for Several Values of Zenith Angle

z (deg)	r (mr)	ρ_{100} (mr)	ρ_{200} (mr)
0	0.00	0.00	0.00
30	0.16	0.036	0.019
50	0.33	0.049	0.025
70	0.77	0.078	0.041

CHAPTER VI

RESULTS AND CONCLUSIONS

As an example of the accuracy obtainable by the analysis techniques discussed, the following sample results are given for rocket "Peggy", 1960 Project Firefly series, center of frame azimuth and elevation for the station at Fort Walton Beach, Florida, from the time of release of the cloud to release plus five minutes.

azimuth 152.925 ± 0.007 (rms) degrees

elevation 60.945 ± 0.009 (rms) degrees

tilt angle -0.29 ± 0.01 (rms) degree

The root mean square deviations in azimuth and elevation correspond to 0.12 and 0.16 milliradian respectively. Taking the square root of the sums of the squares of these deviations yields a total angular rms deviation of ± 0.011 degree or 0.2 milliradian.

The release position of "Peggy" was determined to be

height (km.) 102.93 ± 0.03 (rms)

latitude(deg.) 30.0277 ± 0.0003 (rms) or ± 0.03 km

west longitude(deg.) 86.5213 ± 0.0002 (rms) or ± 0.02 km

Thus the total rms error in position is ± 0.05 km. Since the cloud is at an average distance of 15^4 km from the observing stations, this amounts to an angular error of 0.3 milliradian. This error is typical for cloud points which show up distinctly on the film, so that point identification is not a major source of error.

These values of 0.2 and 0.3 milliradian are about one third of the angular error of 0.8 milliradian quoted by the manufacturer of the K-24 (Vitro, 1954) as obtainable by using individual correction charts supplied with each camera. Thus the accuracy obtainable with the analytic correction procedures discussed here compare favorably with the accuracy obtainable using empirical correction charts.

As an evaluation of the source of the remaining error, let us assume an error in reading the position of a point on the film such that the distance between the measured location of the point and its true location has a magnitude ϵ_r along both the radial line from the center of frame and along a line perpendicular to this. Let us also assume an error ϵ_f in the focal length determination and evaluate the angular error these would produce. This angular error can be calculated with the aid of quantities given in Table 1.

The radial angular error from the focal length inaccuracy would be $\epsilon_f \left| \frac{\Delta\alpha}{\Delta F} \right|$. The error produced by the reading innacuracy would have a radial component of $\epsilon_r \frac{\Delta\alpha}{\Delta R}$, and a component perpendicular to this, ϵ_θ , given by $\epsilon_r \frac{\Delta\phi}{\Delta S}$. The maximum radial angular error ϵ_R would be

$$\epsilon_R = \epsilon_f \left| \frac{\Delta\alpha}{\Delta F} \right| + \epsilon_r \frac{\Delta\alpha}{\Delta R}$$

if the errors are in such directions as to add together. The total angular error, ϵ_t , which is the angle between the measured location of the point and its true location, would be approximately

$$\epsilon_t = (\epsilon_R^2 + \epsilon_\theta^2)^{\frac{1}{2}}$$

If $\epsilon_r = 0.003$ cm and $\epsilon_f = 0.005$ cm and $\left| \frac{\Delta\alpha}{\Delta F} \right|$, $\frac{\Delta\alpha}{\Delta R}$, and $\frac{\Delta\phi}{\Delta S}$ are evaluated at $R = 3$ cm, then ϵ_R would be 0.21 milliradians and ϵ_θ would be 0.16 milliradian, giving an ϵ_t of 0.26 milliradian.

Therefore assuming that the effects of refraction in the glass plate and in the atmosphere, and the effects of film shrinkage and camera tilt have been corrected for exactly, and assuming reasonable values for the error in the focal length and the reading error, we are led to a total angular error which is commensurate with the actual total angular error found.

APPENDIX A

The star images A and B shown in Figure 14 are oriented on the film such that A is to the right of the center of frame, that is $x'_a > 0$, and B is to the left of the center of frame, that is $x'_b < 0$, where x'_a and x'_b are, as before, the x' coordinates of star images A and B on the film. Other possible arrangements of the star images would result from $x'_a > 0$ and $x'_b > 0$, or $x'_a < 0$ and $x'_b < 0$.

In some arrangements of star images the line joining the images A and B would pass above the center of frame, in others this line would pass below the center of frame. In other words, y'_s may be greater than or less than zero, where y'_s is the y' coordinate of the intersection, S, of the line joining A and B with its perpendicular drawn from the center of frame. This is illustrated in Figure 14.

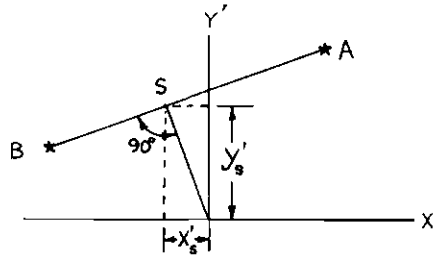


Figure 14. Illustration of the Intersection S and Its y' Coordinates x'_s and y'_s

The value of y'_s is given by

$$y'_s = y'_a - s x'_a - \frac{s^2(y'_a - s x'_a)}{1 + s^2} \quad (71)$$

where s is the slope of line AB in the x' - y' coordinate system given by

$$s = \frac{y'_a - y'_b}{x'_a - x'_b}$$

Formula (71) may be derived by considering the equation of the line AB

$$y' = (y'_a - s x'_a) + s x' \quad (72)$$

The radial distance, r , to any point x' , y' on the line AB is determined by

$$\begin{aligned} r^2 &= (x')^2 + (y')^2 = (x')^2(1 + s^2) + (y'_a - s x'_a)^2 \\ &\quad + 2s(y'_a - s x'_a) x' \end{aligned}$$

To find the x' and y' coordinates of the intersection point S, which is the point where r is a minimum, set $d(r^2)/dx'$ equal to zero.

$$\frac{d(r^2)}{dx'} = 2x'(1 + s^2) + 2s(y'_a - s x'_a) = 0 ,$$

which implies

$$x'_S = - \frac{s(y'_a - s x'_a)}{1 + s^2}$$

Thus y'_s is found by substituting this value of x'_s into (72).

Figures 15 through 20 illustrate the various combinations of values of x'_a , x'_b and y'_s . Accompanying each figure are the relations applicable in that particular case instead of the equations (33) and (37) which apply only in the case illustrated in the text by Figure 10. In Figures 15 through 20 stars A' and B' are shown as they appear on the az-el sphere, Z is the zenith, O' is the point where the extension of the optical axis of the camera meets the az-el sphere, and M' is the point of intersection of line A'B' with the y' axis as it is projected onto the az-el sphere (O'Z). The following generalized definitions of angles apply for all of the figures: ψ_a is angle ZA'O', ν_a is angle ZA'B', ξ_a is angle B'A'O', ψ_b is angle ZB'O', ν_b is angle ZB'A', ξ_b is angle A'B'O', ν'_a is angle ZA'M', and ν'_b is angle ZB'M'.

In addition to illustrating alternate forms for equations (33) and (37), Figures 15 through 20 will serve to illustrate alternate relations for equation (30). The slope y'_x of the line AB between the images of stars A and B on the film is related to angles η_a or η_b . But these angles correspond to angles η'_a and η'_b , shown in Figures 15 through 20 as angles ZM'A' and ZM'B' respectively, η_a and η_b being obtained from η'_a and η'_b by the transformation equation (40) which is derived in Appendix B. The relation between y'_x and η_a or η_b on the film can be deduced from the appearance of angles η'_a and η'_b on the az-el sphere, and from the projection of the x' film axis onto the az-el sphere.

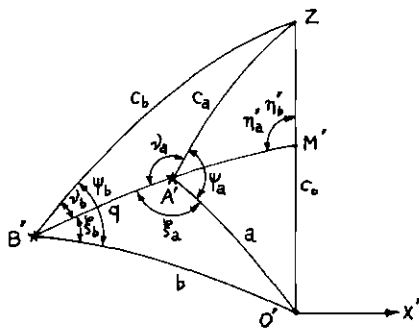


Figure 19. Stars A' and B'
with $y'_s > 0$, $x'_a < 0$, $x'_b < 0$

$$\cos \psi_a = \cos[2\pi - (v_a + \xi_a)]$$

$$= \cos(v_a + \xi_a)$$

$$\cos \psi_b = \cos(v_b + \xi_b)$$

$$y'_x = \tan(\eta_a - \pi/2)$$

$$y'_x = \tan(\eta_b - \pi/2)$$

$$v'_a = \pi - v_a \quad v'_b = v_b$$

$$\cos \psi_a = \cos(v_a + \xi_a)$$

$$\cos \psi_b = \cos[2\pi - (v_b + \xi_b)]$$

$$= \cos(v_b + \xi_b)$$

$$y'_x = \tan(\pi/2 - \eta_a)$$

$$y'_x = \tan(\pi/2 - \eta_b)$$

$$v'_a = v_a \quad v'_b = \pi - v_b$$

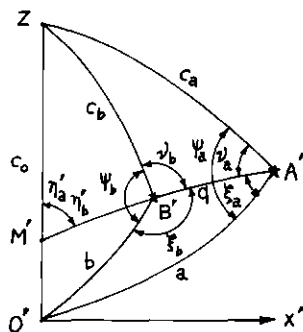


Figure 20. Stars A' and B'
with $y'_s > 0$, $x'_a > 0$, $x'_b > 0$

From the formulas accompanying Figures 15 through 20 the following simplified criteria for determining which of the relations to use are apparent.

$$\begin{aligned} & \cos \psi_a = \cos(v_a + \xi_a) \\ \text{if } y_s' > 0 \end{aligned} \quad (73)$$

$$\cos \psi_b = \cos(v_b + \xi_b)$$

$$\begin{aligned} & \cos \psi_a = \cos(v_a - \xi_a) \\ \text{if } y_s' < 0 \end{aligned} \quad (74)$$

$$\cos \psi_b = \cos(v_b - \xi_b)$$

$$\begin{aligned} & y_x' = \tan(\pi/2 - \eta_a) \\ \text{if } x_a' > 0 \end{aligned} \quad (75)$$

$$v_a' = v_a$$

$$\begin{aligned} & y_x' = \tan(\eta_a - \pi/2) \\ \text{if } x_a' < 0 \end{aligned} \quad (76)$$

$$v_a' = \pi - v_a$$

$$\begin{aligned} & y_x' = \tan(\pi/2 - \eta_b) \\ \text{if } x_b' > 0 \end{aligned} \quad (77)$$

$$v_b' = \pi - v_b$$

$$y'_x = \tan(\eta_b - \pi/2)$$

$$\text{if } x'_b < 0 \quad (78)$$

$$v'_b = v_b$$

Although the above illustrations and conclusions do not constitute a proof of the general validity of the final formulas (73) through (78), these relations should be accurate for any possible arrangement of the star images.

Since it is necessary to employ some of the formulae (73) through (78) before the camera tilt is known, and therefore before the x' and y' coordinates of star images A and B can be determined, it is required that the conditions on x'_a , x'_b , and y'_s be replaced by the similar conditions on x_a , x_b , and y_s . This alteration of the conditions on equations (73) through (78) does not present any difficulty unless the star images A and B are very close to the y axis (i.e. $|x_a|$ and $|x_b| \approx 0$) or unless the line between the images A and B is almost vertical (i.e. $y_s \approx 0$).

APPENDIX B

Figure 21 illustrates schematically the angle η'_a on the az-el sphere and η_a on the film plane. Angle η'_a can be determined by equation (36) in the text. However, it is necessary to know the value of η_a in order to determine the camera tilt. The transformation between η'_a and η_a depends on the angle ω , which is angle ONM ($= O'NM'$). This is angle ω of equation (39) in the text.

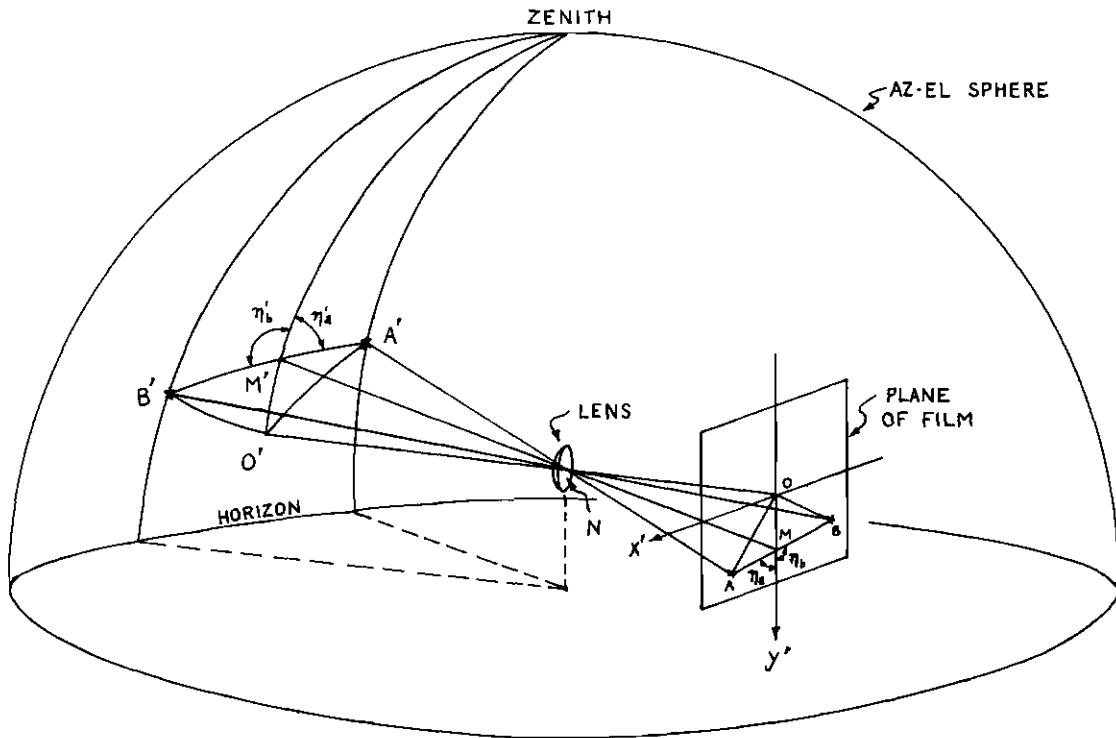


Figure 21. The Angle η'_a on the Az-el Sphere, and the Angle η_a on the Film

Figure 22 shows the necessary geometry for deriving the transformation from η'_a to η_a . In the figure, as in Figure 21, N is the nodal point of the camera lens, M is the intersection of the line AB between the star images and the y axis, O is the intersection of the optical axis of the camera and the film plane, OMS is the y' axis of the film, and A is the image of star A on the film. Line MQ is parallel to the x' axis of the film.

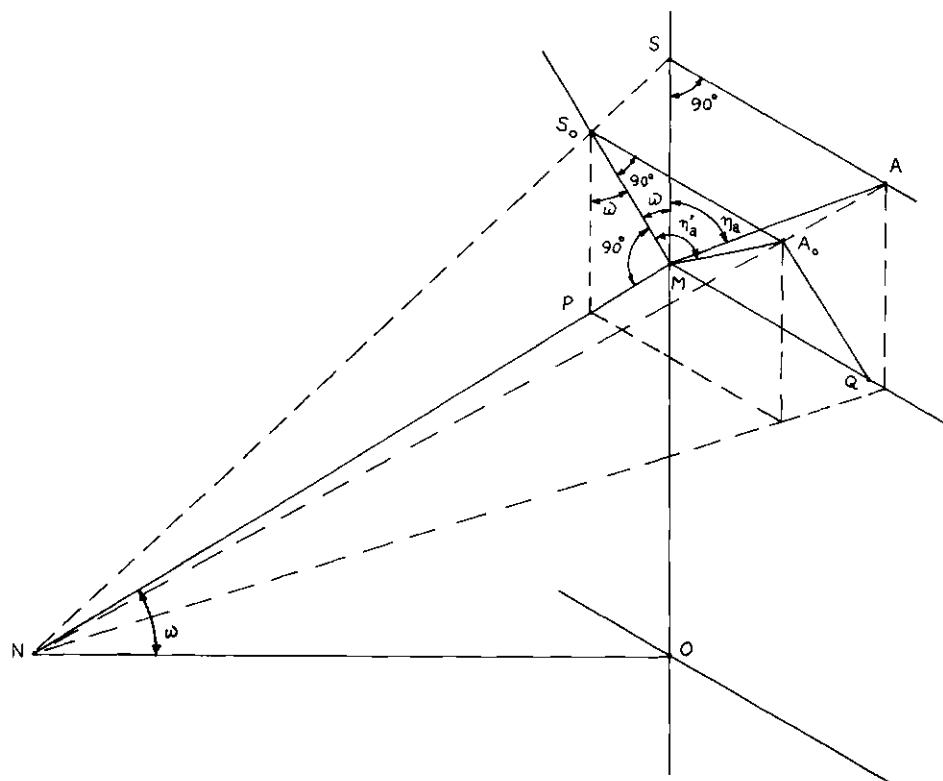


Figure 22. The Geometry of the Transformation of η'_a to η_a

A plane $S_O MQ$ is constructed such that angle SMS_O is equal to ω and $S_O MN$ is 90 degrees. Point A is projected onto this plane, and this projection is called A_O . Angle $S_O MA_O$ is now equal to η'_a because the $S_O MQ$ plane is parallel to the plane tangent to the az-el sphere and perpendicular to line NMM' . Angles ASM and $A_O S_O M$ are right angles.

From Figure 22 it is seen that

$$\tan \eta_a = \frac{AS}{SM} \quad (79)$$

$$\tan \eta'_a = \frac{A_O S_O}{S_O M} \quad (80)$$

From the similar triangles ASN and $A_O S_O N$

$$\frac{AS}{A_O S_O} = \frac{NS}{NS_O} \quad (81)$$

From the similar triangles NSM and $NS_O P$

$$\frac{NS}{NS_O} = \frac{SM}{S_O P} \quad (82)$$

But since angle $MS_O P$ is angle ω

$$S_O P = \frac{S_O M}{\cos \omega} \quad (83)$$

Substituting this into (82) and (82) into (81)

$$\frac{AS}{A_{\circ}S_{\circ}} = \frac{SM}{S_{\circ}M} \cos \omega$$

$$\frac{AS}{SM} = \frac{A_{\circ}S_{\circ}}{S_{\circ}M} \cos \omega \quad (84)$$

but from (79) and (80) equation (84) becomes

$$\tan \eta_a = \tan \eta_a^* \cos \omega \quad (85)$$

which is the transformation equation (40) in the text.

APPENDIX C

As was pointed out in the introduction, the star background is used to determine camera orientation. This is accomplished by calculating the azimuth and elevation of a line of sight along the optical axis of the camera, called the "az-el of the center of frame." All of the quantities necessary for determining the az-el of the center of frame have been arrived at in the text.

The quantity c_o of equation (34) is actually the complement of the elevation of the center of frame, ϵ_o . Therefore ϵ_o is given by

$$\epsilon_o = \pi/2 - c_o \quad (86)$$

The angle ζ_a evaluated by equation (35) is the absolute magnitude of the difference in azimuth between star A and the center of frame. Thus the azimuth of the center of frame α_o is determined from ζ_a and the azimuth of star A, α_a

$$\text{if } x'_a < 0 \quad \alpha_o = \alpha_a + \zeta_a \quad (87)$$

$$\text{if } x'_a > 0 \quad \alpha_o = \alpha_a - \zeta_a$$

where x'_a is the x' coordinate of the image of star A on the film.

Equations similar to (87) would result for star B, using α_b and ζ_b .

BIBLIOGRAPHY

1. Albritton, D. L., L. C. Young, H. D. Edwards, and J. L. Brown;
"Position Determination of Artificial Clouds in the Upper Atmosphere",
Photogrammetric Engineering, September, 1962, p. 608
2. Chauvenet, W.; A Manual of Spherical and Practical Astronomy, (Dover,
1960), Table II, vol II, p. 572
3. Jones, B. L.; "Photogrammetric Refraction Angle: Satellite Viewed
From Earth"; Journal of Geophysical Research; April, 1961; Vol 66;
No. 4; p. 1135
4. Vitro; Instruction Manual KIX 1639, "Operation and Maintenance, K-24
Camera," (1954), p. 27